

- Wildland fire ash enhanced CO₂ flux compared to pre and post-fire soil without ash.
- The addition of wildland fire ash accelerated the recovery of post-fire soil respiration.
- A large fraction of total carbon released occurred shortly after wetting of dry samples.
- Wildland fire ash is a significant player in post-fire carbon fluxes in African savannahs.

1 Wildland fire ash enhances short-term CO₂ flux from soil in a Southern 2 African savannah

3

4 Keywords: vegetation fire; ash; savannah; CO₂ flux; carbon emissions; pyrogenic carbon.

5

6 Abstract

7 Savannah fires are the largest contributor to global carbon (C) emissions from vegetation
8 fires as a result of their high frequency and the large area burnt each year. Fires not only
9 emit CO₂ during the combustion process, they can also lead to enhanced CO₂ fluxes from
10 affected soils and vegetation, especially during the initial post-fire recovery period. Wildland
11 fire ash is a ubiquitous product of vegetation fires known to enrich the nutrient content and
12 pyrogenic C (PyC) of the underlying soil. However, the role of ash in post-fire soil C fluxes has
13 rarely been examined. We address this research gap by investigating the effects of fire and
14 wildland fire ash on CO₂ fluxes from fire-affected savannah soils. Soil and ash material were
15 sampled from three different sites in an African savannah in the Kruger National Park (South
16 Africa) before and immediately after experimental fires. CO₂ fluxes from homogenised
17 natural soils and ash were continuously monitored for 28 days in a laboratory incubation
18 experiment under controlled conditions (20 °C, 60% water-holding capacity). Wildland fire
19 ash enhanced CO₂ emissions by up to 3 times compared with pre- and post-fire soils
20 (without ash), likely as a result of the high content of readily available nutrients in the ash.
21 Our results also show that as much as 40% of the total C released over 28 days occurred
22 during a short-lived burst of CO₂ (lasting between 20 and 61 h) following wetting of the post-
23 fire soil with ash samples. This study, although based on homogenised soil and ash material,
24 shows that not considering wildland fire ash during post-fire soil C observations will likely

25 misrepresent natural conditions and might lead to underestimations of short-term post-fire
26 C fluxes. The large differences observed between the post-fire soil with ash, and both the
27 pre- and post-fire soil without ash, clearly suggest that ash is a key player in C fluxes and
28 should be taken into account in post-fire C cycling studies. Our results also highlight the
29 importance of high frequency observations during the short-term period following wetting
30 of fire-affected soils, since bursts of CO₂ upon wetting of burnt soil can comprise a
31 substantial fraction of total C emissions from burnt savannah soil.

32

33 1. Introduction

34 Fires in savannahs currently represent ~62% of the total global CO₂ emissions from
35 vegetation fires. This is due to their high frequency and the large area burnt annually that
36 these extensive ecosystems exhibit (van der Werf et al., 2017). Fire is a recurrent intrinsic
37 ecological driver in African savannahs and considering that they cover half of the continent,
38 understanding the role of fire in carbon (C) dynamics in these fire-prone ecosystems is
39 essential (Bird et al., 2000; Shackleton & Scholes, 2000).

40

41 Soils store the largest pool of terrestrial C of which approximately two-thirds is soil organic C
42 (SOC; Stockmann et al., 2013). Fire can directly alter the soil C pool by SOC combustion or by
43 modifying SOC characteristics and composition. Indirectly, it can alter processes that affect
44 the fluxes and composition of C, like post-fire changes in vegetation cover and soil erosion
45 (Coetsee et al., 2010; Santín and Doerr, 2018). During a fire some of the burnt biomass is
46 converted into recalcitrant forms of C (known as pyrogenic C, PyC) and can represent a C
47 sink (Santín et al., 2015).

48

49 The CO₂ flux from soils is the largest C flux to the atmosphere from terrestrial ecosystems
50 (Longdoz et al., 2000). Fire can influence soil CO₂ fluxes by reducing microbial activity via
51 heat damage, or by altering soil chemical properties essential for microbial functioning such
52 as nutrient pools (Jensen et al., 2001; Matáix-Solera et al., 2009). Increases in CO₂ fluxes
53 from burnt savannah soils compared with unburnt ones have been observed in response to
54 precipitation events when sufficient soil moisture reactivates microbial activity (Andersson
55 et al., 2004; Castaldi et al., 2010; van Straaten et al., 2019).

56

57 It is widely assumed that ash deposition stimulates soil respiration due to its fertilization
58 effect by supplying readily available nutrients (e.g. Matáix-Solera et al., 2009). Enhanced soil
59 CO₂ fluxes in laboratory-based studies have been reported after the addition of lab-
60 produced ash to burnt soils (Badía & Marti, 2003; Raison & McGarity, 1980) and after the
61 soil fertilization with wood-ash (Fritze et al., 1994; Perkiömaki et al., 2003; Zimmermann &
62 Frey, 2002). In a recent field and laboratory study in a burnt eucalyptus and pine stand in
63 central Portugal we observed a larger increase in the CO₂ flux following wetting of burnt soil
64 in which a surface ash layer was intact compared with burnt soil in which the ash layer had
65 been experimentally removed, but the specific contribution of the ash layer to CO₂ fluxes
66 could not be isolated from other factors such as vegetation cover or soil texture (Sánchez-
67 García et al., 2020). In addition, the ash layer often contains PyC which is relatively resistant
68 to environmental degradation acting as a long-term C sink (Bodí et al., 2014; Santín et al.,
69 2016). Globally, savannah fires are the largest source of PyC because of their high fire
70 frequency (Jones et al., 2019). However, rapid degradation of some forms of PyC has been
71 previously reported from both wildfire-produced PyC (Bird et al., 1999; Zimmermann et al.,
72 2012) and after the application of laboratory-produced PyC to soil (Hilscher et al., 2009;
73 Jones et al., 2011). In some cases, PyC addition has been also observed to have a priming
74 effect in SOC decomposition (Maestrini et al. 2015).

75

76 Although ash is a ubiquitous direct product of vegetation fires, its role in post-fire soil C
77 fluxes has scarcely been considered. This is primarily because of its rapid disappearance
78 from the burnt areas prior to the initiation of most field studies due to its incorporation into
79 the soil or redistribution or loss by wind and water erosion (Bodi et al. 2014; Santín et al.,
80 2012). In addition, differences in the production conditions between naturally-produced ash
81 (thereafter termed 'wildland fire ash') and artificially-produced ash (thereafter termed 'lab
82 ash'), such as the duration of laboratory pyrolysis experiments or oxygen availability, can
83 result in ash of different physico-chemical characteristics (Santín et al., 2017). In this study
84 we refer to 'wildland fire ash' as the particulate ash residue naturally produced during
85 experimental landscape fires (Bodí et al., 2014). To our knowledge, only two previous
86 studies have investigated the input of naturally-produced ash on soil CO₂ fluxes. Enhanced
87 CO₂ fluxes after the input of wildland fire ash were reported from African savannah soils by
88 Andersson et al. (2004); whereas García-Oliva et al. (1999) observed a reduction in CO₂
89 fluxes from soils with added wildland fire ash from a tropical deciduous forest in Mexico
90 suggesting that chemical changes induced by the input of ash inhibited microbial activity.

91

92 Therefore, evidence of the role of wildland fire ash on post-fire C fluxes is sparse and the
93 response of soil CO₂ fluxes to the input of wildland fire ash remains poorly understood. Here
94 we address this knowledge gap and aim at better understanding the effects of savannah
95 fires on CO₂ fluxes from soils. The objective of the study was to investigate the fundamental
96 effects of soil heating and wildland fire ash on CO₂ fluxes from savannah soils. We
97 hypothesised that: I) the input of wildland fire ash to post-fire savannah soil will stimulate
98 CO₂ fluxes, and II) soil heating from the fires will limit biological activity, thus reducing soil
99 CO₂ flux when compared with pre-fire soil.

100

101 2. Research design and methods

102 2.1. Study sites

103 The study comprises a series of CO₂ flux incubation experiments on homogenised natural
104 soil and ash materials (< 2 mm fraction) conducted under controlled laboratory conditions.
105 Samples were collected hours before (pre-fire soils) and after (post-fire soils and ash) large-
106 scale experimental fires conducted in the Kruger National Park (KNP; South Africa) in August
107 2018, in the middle of the dry season. The locations used for the study are part of the
108 ongoing long-term experimental burn plots (EBPs) at KNP established in 1954 to study the
109 impact of different fire regimes across representative South African savannah landscapes
110 (Biggs et al., 2003). Three plots were selected for the study. Two of the plots were located in
111 the Pretoriuskop area (mean annual rainfall of 705 mm), a Lowveld Sour Bushveld landscape
112 on sandy granitic soils, which included one plot burnt annually (hereafter known as PB1;
113 lat./long.: 25° 08' 24''S; 31° 12' 26''E) and a second plot burnt triennially (hereafter known
114 as PB3; lat./long.: 25° 08' 06''S; 31° 12' 24''E). The dominant grass species were *Hyperthelia*
115 *dissoluta*, *Themeda triandra* and *Setaria sphacelata*. The main tree species were
116 *Dichrostachys cinerea* and *Terminalia sericea*. The third plot was located in the Mopani area
117 (mean annual rainfall of 451 mm), a *Colophospermum mopane* shrubveld on clayey basaltic
118 soil, which has been burnt annually (hereafter known as MB1; lat./long.: 23° 33' 48''S; 31°
119 27' 24''E). The dominant grass species was *Bothriochloa radicans* and the dominant tree
120 species was *Colophospermum mopane*.

121

122 2.2. Experimental fires and soil and ash sampling

123 For soil and ash sampling and fire behaviour monitoring, a 30 x 30 m subplot was selected
124 within the experimental burn plot at both PB1 and PB3 (Fig. 1c). These subplots were
125 located more than 20 m from the edge of the burn plots to avoid edge effects (Smit & Asner,

126 2012). Locating a subplot with enough fuel continuity to ensure a successful burn was
127 challenging in MB1, therefore, a smaller subplot of 20 x 20 m with sufficient fuel was
128 selected (Fig. 1c). Before conducting the fires, three parallel transects were established
129 within each plot, 30 m long and 15 m apart in PB1 and PB3, and 20 m long and 5 m apart in
130 MB1. To monitor temperatures during the fire, K-type thermocouples with dataloggers
131 (Lascar, Easylog) were installed along each transect at four sampling points, at 9 m intervals
132 in PB1 and PB3 and 5 m intervals in MB1. At each sampling point (n = 12 per plot: Fig. 1c),
133 one thermocouple was placed in the grass, 3 – 5 cm above the ground, and another in the
134 mineral soil at ~1 cm below the surface. In addition, between the three sampling transects,
135 two ‘control’ transects were used for taking soil samples before the fire without disrupting
136 the post-fire sampling transects (Fig. 1c). A couple of hours before the fire, the top 0 - 1 cm
137 soil layer was sampled along these ‘control’ transects at 3 m intervals in PB1 and PB3 and
138 1 m intervals in MB1 (n = 20), using a 20 x 20 cm sampling frame and after removal of the
139 grass. The same day of the fire, the ash layer was brushed off the surface and the top 0 –
140 1 cm soil layer was sampled along the three sampling transects at the same points where
141 the thermocouples had been placed (n = 12) also using a 20 x 20 cm frame. At each plot,
142 three composite ash samples were also taken, based on material collected from several
143 locations within each burnt plot (approximately 500 g per sample). All samples were air
144 dried and stored in dry conditions in the laboratory. The fire characteristics are given in
145 Table 1. [Fig. 1 and Table 1 should be near here]

146

147 2.3. Laboratory experiments and analysis

148 2.3.1. CO₂ flux

149 For the laboratory experiments, the following sample materials were used from each of the
150 three burn plots: a) a pre-fire composite soil sample per site formed by combining equal

151 weights of the samples collected before the fire from each site ($n = 20$); b) a post-fire
152 composite soil sample per site formed by combining equal weights of the samples collected
153 after the fire from each sampling location ($n = 12$) and c) a composite ash sample per site
154 formed by combining the three ash samples. All air-dried soil and ash samples were sieved
155 to < 2 mm to remove larger debris. To study the effect of fire and the impact of naturally-
156 produced ash (wildland fire ash) on CO_2 fluxes, we used the following treatments: pre-fire
157 soil (PreF), post-fire soil without ash (PostF) and post-fire soil with added ash (PostF_wA).
158 We included three replicates of these three treatments from each site (PB1, PB3 and MB1),
159 resulting in 27 separate samples for flux measurement. The 70 g of soil material for the PreF
160 and PostF treatment were carefully placed into gas-tight plastic containers of 9 cm diameter
161 and 11 cm height. For the post-fire soil with added ash (PostF_wA), 7 g of ash was mixed
162 with 70 g of post-fire soil from their respective plots to create homogeneous samples. The
163 ash load (1051 g m^{-2}) was substantially higher than that observed in the field ($\sim 90 \text{ g m}^{-2}$,
164 unpublished data), but selected in order to be comparable with other PyC/ash-soil
165 incubation studies (e.g. Gómez-Rey et al., 2012; Smith et al., 2010; Whitman et al., 2016).
166 The CO_2 flux measurements were conducted by connecting each soil container to an infrared
167 CO_2 gas analyser system (IRGA) (Li-8100A, Li-COR Inc., Lincoln, NE, USA) via a multiplexer (Li-
168 8150, Li-COR Inc., Lincoln, NE, USA) to allow an automated measurement of the CO_2 flux
169 from each sample every hour. Ambient air was continuously flushed between
170 measurements to prevent high CO_2 concentrations from developing in the containers. The
171 measurement of the CO_2 concentration in each container lasted 2 min with an additional
172 30 s for pre- and post-purge. The measurements of the soil CO_2 flux for the first 24 h started
173 with air-dried samples. The initial soil moisture in the air-dried samples (i.e. 1.3%, 1.7% and
174 2% gravimetric SWC for the PB1, PB3 and MB1 respectively) was lower than that typically
175 observed under field conditions during the dry season, when soil moisture typically ranges
176 between 3 – 5% across the KNP (Table 1 and Khosa et al., 2020). The samples were then

177 wetted to 60% of water-holding capacity (WHC) to ensure moisture availability while
178 avoiding saturation. The wetting was achieved by spraying deionised water from above. The
179 CO₂ flux monitoring was continued for 28 days. Soil moisture (60% WHC; i.e. 10% and 18%
180 volumetric soil water content for the PB and MB1 soils, respectively) and temperature
181 (~20 °C) were maintained throughout the observations, with any minor moisture loss caused
182 by evaporation being adjusted daily according to the weight difference in the samples from
183 the previous day. A small number of shoots that germinated from the soil during the
184 incubations were quickly removed by clipping to eliminate any root and shoot respiration.

185

186 The CO₂ concentration data over time was fitted exponentially, excluding the initial 30 s. Any
187 CO₂ flux data ($\mu\text{mol m}^{-2} \text{s}^{-1}$) with a coefficient of $R^2 \leq 0.95$ was discarded. This applied to < 3%
188 of the total measurements, which correspond predominantly to dry soil before wetting
189 where the CO₂ flux was 0, or close to 0. Therefore, discarding these values does not affect
190 the results. The cumulative flux ($\mu\text{mol m}^{-2}$) was calculated as the total CO₂ flux emitted
191 during the whole duration of the observations (28 d). Carbon respired was calculated by
192 converting cumulative flux ($\mu\text{mol m}^{-2}$) to g C m^{-2} .

193

194 2.3.2. Chemical Analysis

195 The pH and electrical conductivity (EC) of soil and ash samples were determined in water at
196 a soil/ash-to-water mass ratio of 1:2.5 after stirring and waiting for 10 min (Buurman et al.,
197 1996). pH was measured with a Crison micropH 2000 pH meter, with buffer solutions of pH
198 4, 7 and 9. EC was measured with a Crison GLP 31 apparatus, calibrated with 0.1 and 0.01 M
199 potassium chloride (KCl) solutions (12.88 mS cm^{-1} and $1413 \mu\text{S cm}^{-1}$, respectively).

200

201 Total Nitrogen (TN) and carbon (TC) concentrations were determined using a Leco TruSpec
202 CHN. The total concentration of aluminium (Al), calcium (Ca), cobalt (Co), chromium (Cr),
203 copper (Cu), iron (Fe), magnesium (Mg), manganese (Mn), nickel (Ni) and zinc (Zn) were
204 determined in extracts obtained by acid digestion (HNO_3/HCl , ratio v/v 3:1; at 180 °C for
205 45 min in an Ethos Easy Milestone Microwave) and measured by Atomic Absorption in a
206 PerkinElmer PinAAcle 500 Atomic Absorption Spectrometer. Total phosphorus (P) was
207 measured in the same extracts by colourimetry in a Jasco V360 spectrophotometer.

208

209 Water-soluble elements were extracted following the leaching test method described in
210 Hageman (2007). Two g of sample were weighed into 50 ml bottles. Then, 40 ml ultrapure
211 water (sample:water ratio 1:20) was added and the bottles were capped and shaken for
212 5 min. After shaking, the contents were allowed to settle for 10 min. The supernatants were
213 vacuum-filtered through 0.45 μm cellulose nitrate membranes. Water-soluble organic
214 carbon (WSOC), phosphate (PO_4^{3-}) and ammonium (NH_4^+) were then measured by
215 colourimetry in a Jasco V360 spectrophotometer. Water-soluble nitrate (NO_3^{-2}) was
216 quantified by liquid ion chromatography (Dionex Series 4500i Chromatographer).

217

218 2.3.3. TG-DSC analysis

219 Thermogravimetry-Differential Scanning Calorimetry (TG-DSC) was performed in order to
220 examine thermal recalcitrance in the soil and ash material. The analyses were conducted in a
221 simultaneous Thermal Analyzer (STA) 6000 PerkinElmer. Ground samples (50-70 mg) were
222 placed in a ceramic crucible and heated under dry air (under O_2 flux; flow rate, 50 mL^{-1}) with
223 increasing temperature from 50 to 600 °C at a heating rate of 10 °C min^{-1} while continuously
224 monitoring the combustion rate and sample mass change rate. For each DSC thermograph,
225 the area in the 150 - 600 °C region, where the combustion of organic matter (OM) occurs,

226 was divided into three temperature sections representing different levels of resistance to
227 thermal oxidation (Merino et al., 2015): labile OM, mainly comprising carbohydrates,
228 proteins and other labile aliphatic compounds ($150 < T1 < 375$ °C); recalcitrant OM, such as
229 lignin or other polyphenols ($375 < T2 < 475$ °C); and highly recalcitrant OM, such as
230 polycondensed aromatic forms ($475 < T3 < 600$ °C). The resulting partial heats of
231 combustion, representing these three regions were calculated as Q1, Q2 and Q3,
232 respectively.

233

234 2.4. Data analysis

235 The non-parametric Mann-Whitney U-test was used to test for statistical differences in the
236 CO₂ fluxes (accepted at $p < 0.05$) between the incubation treatments and to test for
237 differences in chemical composition and thermolability. The Spearman's rank correlation
238 coefficient (ρ) was used to test for linear correlations between the CO₂ flux and chemical
239 properties (significance level set at $p < 0.05$). The tests were performed with Microsoft Excel
240 2011. The correlation tests amongst the thermogravimetry indicators and CO₂ fluxes were
241 not performed since thermogravimetry data for the PostF_wA treatment were not available,
242 as these were only obtained for the post-fire soil and the ash samples individually.

243

244 3. Results

245 3.1. CO₂ flux evolution with time

246 For all samples, the CO₂ flux before wetting was below $0.1 \mu\text{mol m}^{-2} \text{s}^{-1}$. Following wetting,
247 the CO₂ flux increased in all samples (i.e. PreF, PostF and PostF_wA) after a lag phase of 14
248 to 23 h in the PB1 and PB3 soils and ~29 h in the MB1 soil (Fig. 2). With the addition of ash to
249 the post-fire soil (PostF_wA) the lag phases in the PB1, PB3 and MB1 soils were 8, 9 and 25 h

250 shorter than in the pre-fire soil, respectively. After the lag phase the CO₂ fluxes quickly
251 reached a peak (between 1 and 29 h) in all samples, except in the MB1 PreF soil where no
252 distinct peak was detected (Fig. 2). The CO₂ pulse in pre-fire (PreF) soils was low (mean $\leq 1 \pm$
253 $0.18 \mu\text{mol m}^{-2} \text{s}^{-1}$), while post-fire (PostF) soils had a significantly higher pulse ($p < 0.001$)
254 with the mean ranging between 1.5 ± 0.08 and $2.5 \pm 0.24 \mu\text{mol m}^{-2} \text{s}^{-1}$ in the PB1 and PB3
255 soils, respectively (Fig. 2). [Fig. 2 should be near here]

256

257 The addition of ash to the post-fire soils (PostF_wA) resulted in an even higher pulse in all
258 samples ($p < 0.001$), reaching a mean of $4.5 \pm 0.8 \mu\text{mol m}^{-2} \text{s}^{-1}$ in the MB1 soil and 3.5 ± 0.19
259 and $3.3 \pm 0.14 \mu\text{mol m}^{-2} \text{s}^{-1}$ in the PB1 and PB3 soils (Fig. 2). The size of the pulse in the PB1
260 and PB3 PostF_wA soils was triple that of the PreF and nearly 11 times higher in the MB1
261 PostF_wA than in the PreF. The CO₂ fluxes decreased quickly after reaching their peak and
262 the pulse was over within the following 34 to 130 h. The CO₂ fluxes remained low thereafter
263 ($< 0.5 \mu\text{mol m}^{-2} \text{s}^{-1}$) in all soils until the end of the observations, 27 d after the beginning of
264 wetting (Fig. 2).

265

266 3.2. Cumulative CO₂ flux and respired C

267 The cumulative CO₂ flux in the PreF soils ranged between 594 and 869 mmol m⁻² in the PB3
268 and MB1 soil, respectively (Fig. 3). In the PostF soils, the cumulative flux was 25, 36 and 97%
269 higher than in the PB1, MB1 and PB3 PreF soils, respectively ($p < 0.001$; Fig. 3). The addition
270 of ash to the post-fire soils (PostF_wA) doubled the cumulative flux of the PreF soils in the
271 PB1 and MB1 (mean 1707 ± 98 and $1718 \pm 66 \text{ mmol m}^{-2}$, respectively) and trebled PreF
272 values in the PB3 soil (mean $1772 \pm 56 \text{ mmol m}^{-2}$; $p < 0.001$). The total C released from the
273 PostF_wA soil comprised 3 - 5% of the total carbon (TC) present in the sample (soil + ash)
274 (Table 2). [Fig. 3 and Table 2 should be near here]

275

276 The cumulative flux released during the pulse only comprised up to 23% of the total
277 cumulative flux in the PreF soils (up to 1% of the TC) (Table 2). Up to 36 and 41% of the total
278 cumulative flux was released during the pulse in the PostF and PostF_wA respectively,
279 accounting for up to 3% of TC in the PostF soil and up to 2% of TC in the PostF_wA soil (Table
280 2).

281

282 The cumulative flux was positively correlated to dissolved organic carbon (DOC) and total
283 carbon (TC; Fig. 4). The size of the CO₂ pulse was significantly correlated to cumulative CO₂
284 flux, TC, DOC and NH₄⁺. TC was significantly correlated to TN and PO₄⁻³, and TN was
285 significantly correlated to NO₃⁻² (Table 3). [Fig. 4 and Table 3 should be near here]

286

287 3.3. Chemical properties of soil and ash

288 Statistically significant differences were observed between PreF and PostF soils in the three
289 studied sites in pH, electrical conductivity (EC), dissolved organic carbon (DOC), water-
290 soluble ammonium (NH₄⁺), nitrate (NO₃⁻²), phosphate (PO₄⁻³), total chromium (Cr), copper
291 (Cu) and phosphorus (P). After the fire, a significant increase was found in both pH (from 6.5
292 to 7.5) and water-soluble PO₄⁻³ (from 0.4 to 2.3) in the PB3 soil (Table 4). With regards to
293 DOC, a significant increase was detected in all PostF soils, which was particularly prominent
294 in the MB1 soil where DOC values were 5 times higher than PreF ones (8.4 to 13.7 mg kg⁻¹ in
295 the PB1 soil, 5.0 to 27.2 mg kg⁻¹ in the PB3 soil and 5.7 to 19.4 mg kg⁻¹ in the MB1 soil, Table
296 4). While the concentration of water-soluble NH₄⁺ was significantly enhanced after the fire in
297 the PB3 soil (from 0.1 to 0.6 mg kg⁻¹); the concentration of water-soluble NO₃⁻ increased
298 (from 0.4 to 0.8 mg kg⁻¹) and decreased (1.5 to 0.9 mg g⁻¹) significantly in the PB1 and MB1
299 soil after fire, respectively (Table 4). [Table 4 should be near here]

300

301 Regarding the ash samples, pH values were consistently around 10 (Table 4). The TC ranged
302 between 20,900 and 28,600 mg kg⁻¹ in the PB3 and MB1 sites respectively. The TN in the
303 MB1 ash was nearly half that in the PB1 ash and around a third lower than in the PB3 ash
304 (Table 5). Regarding inorganic N, both the concentrations of water-soluble NH₄⁺ and NO₃⁻²
305 were significantly higher in the PB1 and PB3 soils than in the MB1 soils. The concentration of
306 water-soluble PO₄⁻³ was especially high in the ash from the MB1 site with an average of 149
307 mg kg⁻¹ compared with 6.7 and 6.2 mg kg⁻¹ in the PB1 and PB3 sites (Table 4). [Table 5 should
308 be near here]

309

310 3.4. Differential scanning calorimetry (DSC) and thermogravimetry (TG) analysis

311 The DSC thermographs of the pre-fire samples revealed a first peak (T_{1Q}) in the range of 346
312 – 353 °C and a second, less prominent peak (T_{2Q}) at 376 – 399 °C (Fig. S1). In the pre-fire
313 samples the majority of the energy was released in the Q1, which represents the labile OM
314 category (Table 6; Campo & Merino, 2016). [Table 6 should be near here]

315

316 The thermograms of the soils sampled after the fire maintained the shape of the pre-fire
317 samples with a peak at 341 – 346 °C (Fig. S1). T_{50Q} rose slightly but not significantly in both
318 the PB1 and PB3 soil after the fire (371 - 388 °C in the PB1 soil and 304 - 355 °C in the PB3
319 soil), and did not differ from pre-fire values in the MB1 soil (Table 6). The Q1 thermolability
320 remained the most dominant category for all three soils (Table 6).

321

322 The DSC thermograms of the ash samples showed a prominent peak at much higher
323 temperatures than in the soil samples, around 438 – 464 °C (Fig. S1). Most of the OM in the
324 ash samples was classified into the Q2 category (43 - 56%), representing recalcitrant OM,

325 with only 21 - 29% of the DSC thermogram's area in the labile Q1 category. The ash from the
326 PB1 site showed the highest thermolability (Q1 = 29% and Q3 = 15%) while the lowest
327 thermolability was observed in the MB1 site (Q1 = 21% and Q3 = 25%; Table 6). Detailed
328 values of the TG-DSC analysis are shown in Table S2.

329

330 4. Discussion

331 4.1. CO₂ flux responds to ash input but not to soil heating

332 The post-fire soils showed an increase in CO₂ flux for all samples within 3 to 29 h after the
333 start of the wetting. The additional input of wildland fire ash stimulated this CO₂ release by 2
334 to 3 times compared with the pre-fire and post-fire soils (without ash; Fig. 3). Therefore, we
335 accept our first hypothesis that the input of wildland fire ash to fire-affected savannah soil
336 stimulates soil CO₂ flux. Enhanced CO₂ fluxes following wetting of fire-affected soils have
337 been previously reported either during rainfall simulation experiments (e.g. Pinto et al.,
338 2002; Castaldi et al., 2010), or after actual rainfall events (e.g. Pinto et al., 2002; van
339 Straaten et al., 2019). In a previous field study we also observed a rapid increase in the CO₂
340 flux following a rainfall simulation in a recently burnt pine and eucalyptus stand in Portugal,
341 and larger CO₂ fluxes in plots with ash compared with those in which the ash layer was
342 removed, although the specific effect of ash could not be isolated from that of vegetation
343 cover and soil texture (Sánchez-García et al., 2020). Enhanced soil CO₂ fluxes with the
344 experimental addition of ash have also been observed in previous incubation studies (e.g.
345 Badía and Marti, 2003; Raison and McGarity, 1980; Hogg et al., 1992). For example, in the
346 incubation experiment by Badía & Marti (2003), a 10% increase in respiration was observed
347 with the addition of laboratory-produced ash to artificially-burnt soils from NE-Spain. Our
348 results are in line with Andersson et al. (2004) who, to our knowledge, conducted the only
349 previous study isolating the effects of wildland fire ash on C fluxes. They reported higher CO₂

350 fluxes in burnt loamy soils with added wildland fire ash than in burnt-only soils from African
351 savannah woodland during a field experiment.

352

353 Ash is rich in organic C and soluble nutrients readily available for mineralization, like N and P
354 (Tables 4 and 5; Bodí et al., 2014). The high pH commonly observed in ash (~10 in this study)
355 can reduce soil acidity and enhance nutrient availability (Jensen et al., 2001; Perkiömaki et
356 al., 2003). This can boost microbial activity resulting in higher respiration rates (Fritze et al.,
357 1994; Zimmermann & Frey, 2002). Although carbonates present in the ash can contribute to
358 the rapid CO₂ release upon wetting (Serrano-Ortiz et al., 2010), the addition of hydrochloric
359 acid to the ash from this study showed no presence of carbonates. Therefore, we expect the
360 contribution from carbonates in the ash to CO₂ fluxes here to be negligible.

361

362 It is important to note that for our results to be replicable we produced homogeneous
363 samples of the post-fire soil with ash. However, under natural conditions the effect of ash
364 can be spatially heterogeneous since some ash will be redistributed by wind and water and
365 likely accumulate preferentially in depositional areas in the landscape, or be incorporated in
366 the soil by bioturbation or percolating rainfall (Bodí et al., 2014).

367

368 Our results indicate that heating from the fire had little direct impact on the soil as
369 supported by the slight and non-significant differences in thermal recalcitrance between
370 pre- and post-fire soils (Table 6) and the generally low temperatures registered in the soil
371 surface during the fires (Supplementary Table 1). Thus, we can reject our second hypothesis
372 that heating of savannah soil reduces CO₂ flux when compared with pre-fire soil. Lower CO₂
373 fluxes were emitted from the post-fire soils without ash than from post-fire soils with ash,
374 but the former were still significantly higher than those emitted from the pre-fire soils. This

375 is likely a result of some residual ash being incorporated in the post-fire mineral soil surface
376 sampled after the removal of the ash layer (Fig. 1).

377

378 The average CO₂ fluxes observed in the post-fire soil with wildland fire ash are similar to
379 those in unburned savannahs reported by Zepp et al. (1996), who observed mean fluxes
380 (measured for 30 min per day) of ~1 g C m⁻² d⁻¹ after light *in-situ* wetting of the soil in a semi-
381 arid savannah also from the Kruger National Park. Our daily flux in the post-fire soil with
382 added ash averaged 0.8 g C m⁻² d⁻¹. In contrast, the CO₂ flux reported in our post-fire soil
383 with wildland fire ash is lower than those reported by Castaldi et al. (2010) (10 g C m⁻² d⁻¹,
384 fluxes measured 5 times over a two-week period) and Pinto et al. (2002) (3.7 g C m⁻² d⁻¹,
385 fluxes measured 3 times during one month); both during *in-situ* observations in a grass and
386 shrub savannah in the region of Congo (central Africa) and in a Brazilian savannah (central
387 Brazil), respectively. When compared with other arid and semi-arid ecosystems the mean
388 CO₂ flux observed in our post-fire soil with added ash is similar to those reported by Vargas
389 et al. (2012) (between 0 and 1 μmol m⁻² s⁻¹) following a wildfire in an arid grassland in New
390 Mexico (USA) receiving 20 mm per month of rainfall. In wildfire-burnt semi-arid mixed
391 conifer and ponderosa pine stands in Oregon, Meigs et al. (2009) and Irvine et al. (2007)
392 reported higher annual CO₂ fluxes (~300 g C m⁻² y⁻¹ in both cases), but in the same order of
393 magnitude as those estimated for this study. In contrast, double the mean CO₂ fluxes (~2 g
394 CO₂ m⁻² d⁻¹) as those observed in this study (~0.8 g C m⁻² d⁻¹) were reported by Wüthrich et
395 al. (2002) over the month following an experimental fire in a sweet chesnut forest in
396 southern Switzerland.

397

398 From all the analysed chemical parameters total CO₂ released from the samples was only
399 positively correlated to TC and DOC (Table 3). Similar relationships with TC and DOC were
400 reported by Dicen et al. (2020) and Badía and Marti (2003), respectively, in their laboratory

401 incubation studies using artificially-burnt soil. Ash is a very good source of easily
402 mineralizable C (Table 4) and it is likely that microorganisms initially rely on the DOC, since
403 this C pool can be accessed immediately (Jones et al., 2011), after which microbes will utilise
404 more stable forms of C (Hilscher et al., 2009). However, the DOC in our samples (≤ 0.002 g C
405 in all cases, data not shown) is an order of magnitude lower than the total C respired (Table
406 2). Another explanation could be that microorganisms do not directly mineralize the labile C
407 in the ash, but use the nutrients in the ash to mineralize C from the native soil organic
408 matter (priming effect) (Maestrini et al., 2015).

409

410 The organic carbon in vegetation fire ash is mostly present in the form of PyC (Santín et al.,
411 2020). Even though PyC is considered highly resistant to microbial degradation, it has a labile
412 component (relatively large in our samples, between 21 and 29%, as indicated by the Q1% in
413 Table 5) which can undergo fairly rapid degradation during the initial stages of
414 mineralisation (Santín et al., 2016). High wildfire PyC degradation rates have previously been
415 reported in savannah soils from Zimbabwe (Bird et al., 1999) and Australia (Zimmerman et
416 al., 2012). Similarly, during a laboratory incubation experiment, Hilscher et al. (2009)
417 observed a complete consumption of the PyC's labile fraction (lab-produced) within the
418 initial 30 days of the incubation.

419

420 The results from this study clearly show that examining post-fire soil without ash is unlikely
421 to reflect natural conditions except for those patches in which ash has been lost by wind or
422 water erosion. It is important to highlight that the ash load applied in this study was
423 substantially higher than that generated from the experimental burns in the field in order to
424 allow comparison with previous PyC/ash-soil incubation studies. The outcomes should thus
425 be seen as indicative only, and we expect the CO₂ flux response to be less pronounced under
426 field conditions due to this factor and post-fire ash redistribution.

427

428 4.2. Ash accelerated the CO₂ flux recovery after fire

429 The CO₂ pulse observed after wetting was preceded by a lag phase of very low CO₂ flux
430 lasting between 14 to 29 h (Fig. 2). Rewetting of dry soils is associated with a large flush of
431 CO₂ from the soil, known as the Birch effect (Birch, 1958), and has been extensively
432 observed in burnt and unburnt soils (Jarvis et al., 2007; Sánchez-García et al., 2020; Thomas
433 et al., 2014). In burnt soils the duration of the lag phase (i.e. the microbial activity recovery
434 time after the fire) is linked to heat exposure, since soil temperatures > 80 °C may kill many
435 microorganisms with most of them disappearing completely at 115 – 150 °C (Matáix-Solera
436 et al., 2009). During the experimental fires in this study only a few points registered T_{max} >
437 80 °C (Supplementary Table 1); therefore, considering that our studied samples were
438 composite samples, we expect that heating did not lead to high rates of microbial mortality
439 in our soils. This suggests that the lag phase is likely a consequence of the dry conditions
440 before wetting. These observations are in line with Pinto et al. (2002) and Zepp et al. (1996)
441 who also observed very low or negligible effects of fire on CO₂ fluxes. The length of the lag
442 phase observed in this study is in line with those reported following wetting of dry unburnt
443 soil (e.g. Meisner et al., 2017; Göransson et al., 2013).

444

445 Shorter lag phases were observed in all the post-fire soils with added ash; likely in response
446 to the input of readily available nutrients from the ash (Fig. 2). An exceptionally short lag
447 phase of only 3 h was observed in the MB1 post-fire soil with ash along with a higher CO₂
448 pulse than in the other two soils. The MB1 soil exhibited higher nutrient content than both
449 PB soils (Table 4 and 5) which could lead to a quicker recovery of microbial activity. Yet no
450 differences in the duration of the lag phase were observed amongst the pre- and post-fire
451 soil without ash in this soil. The very short lag phase in the MB1 post-fire soil with ash may

452 have been a response to the high available P in the ash from this site (i.e. water soluble PO_4^{3-}
453 3 ; Table 5). P is one of the most limiting nutrients in savannahs (Feig, 2004). Large inputs of P
454 can result in its adsorption to soil particles and the desorption of bonded OM, which can
455 increase the amount of DOC within 1 h after the addition of P and contribute to the larger
456 CO_2 pulse (Meisner et al., 2015; Spohn & Schleuss, 2019). The increase in available P might
457 also accelerate the reactivation of heterotrophic bacteria in soil which generally recovers
458 quickly after a fire (Matáix-Solera et al., 2009) and could be a contributing factor for the
459 quick and large CO_2 pulse in the MB1 soil after the addition of ash.

460

461 4.3. The importance of capturing the CO_2 flux response to wetting

462 The high-temporal resolution of our observations shows that up to 40% of the total C
463 respired from post-fire soils with ash occurred within hours after the wetting. In African
464 savannahs the CO_2 flux emitted during pulses in response to rainfall is estimated to account
465 for up to a fifth of the annual CO_2 flux from soils (Fan et al., 2015) and soil moisture is one of
466 the main CO_2 flux controllers in these semi-arid ecosystems (Zepp et al., 1996). In this study
467 the burst of CO_2 following wetting of fire-affected soil was highly enhanced by wildland fire
468 ash. After a fire the first wetting mobilises soil nutrients from both the soil and ash,
469 reactivates microbial activity and facilitates the release of stored CO_2 in the soil pores
470 resulting in a short, yet intense, mineralisation period which would explain the large CO_2
471 flush observed in this study (Matáix-Solera et al., 2009; Sánchez-García et al., 2020).

472

473 It is unlikely that under field conditions soil moisture would remain constant for long periods
474 of time following wetting of burnt soil (e.g. Vargas et al., 2012). Instead another period of
475 dry weather might follow with subsequent fluctuation in the CO_2 fluxes after each drying-
476 wetting cycle. Capturing these “hot moments” of CO_2 release after a wildfire, and while the

477 layer of ash is still on the soil surface, is challenging but missing these large spikes in CO₂ flux
478 can lead to unrealistic estimates of post-fire C dynamics and highlights the need to (i)
479 increase the frequency of observations and (ii) for models to reflect this high variation in CO₂
480 fluxes. This becomes especially relevant in ecosystems with high fire frequency, like
481 savannahs, which contribute most to global CO₂ emissions from vegetation fires each year
482 (van der Werf, et al., 2017), and where fire occurrence is already being altered by climate
483 change (Zubkova et al. 2019; Wei et al., 2020).

484

485 In summary, this study indicates that ash plays a quantitatively important role in post-fire C
486 emissions. We expect a similar response of soil C fluxes to the presence of wildland fire ash
487 in other post-fire environments, but the magnitude of this response, which we anticipate
488 will depend on factors including fire characteristics, vegetation and soil types, and climatic
489 conditions during the post-fire period, needs to be assessed by future studies.

490

491 [Acknowledgments](#)

492 CSG and EU were supported by the Royal Society – Research Grants for Research Fellows
493 (RG120366), Research Fellows Enhancement Award (RGF\EA\180262) and Dorothy Hodgkin
494 Fellowship (DH110189), all awarded to EU. CS and SD were supported by the Leverhulme
495 Trust Research Grant (RPG-2014-095) and the European Union's Horizon 2020 Research and
496 Innovation Programme under the Marie Skłodowska-Curie Grant Agreement 663830. CS also
497 received funding from the Spanish 'Ramon y Cajal' programme, Ref. N. RYC2018-025797-I.
498 Ash analyses were supported by Natural Environment Research Council grant
499 (NE/R011125/1). We would like to thank the Scientific Services (Kruger National Park) Fire
500 Team for applying the experimental fires which enabled this research to be conducted.
501 Approval to conduct this study within Kruger National Park was granted as part of a

502 registered research project (Research Code: SANTC1488) with a signed research agreement
503 between South African National Parks and the research team. We are grateful to Maria
504 Santiso for the thermogravimetry and chemical analysis and to Julia Kelly for proofreading of
505 the manuscript.

506

507 References

508 Andersson, M., Michelsen, A., Jensen, M., Kjøller, A. (2004). Tropical savannah woodland:

509 Effects of experimental fire on soil microorganisms and soil emissions of carbon
510 dioxide. *Soil Biology and Biochemistry*, *36*, 849–858.

511 <https://doi.org/10.1016/j.soilbio.2004.01.015>

512 Badía, D., Martí, C. (2003). Effect of simulated fire on organic matter and selected

513 microbiological properties of two contrasting soils. *Arid Land Research and*

514 *Management*, *17*, 55–69. <https://doi.org/10.1080/15324980301594>

515 Biggs, R., Biggs, H. C., Dunne, T. T., Govender, N., Potgieter, A. L. F. (2003). Experimental

516 burn plot trial in the Kruger National Park: History, experimental design and

517 suggestions for data analysis. *Koedoe*, *46*, 1–15.

518 <https://doi.org/10.4102/koedoe.v46i1.35>

519 Birch, H. F. (1958). The effect of soil drying on humus decomposition and nitrogen

520 availability. *Plant and Soil*, *10*, 9–31. <https://doi.org/10.1007/BF01343734>

521 Bird, M. I., Moyo, C., Veenendaal E. M., Frost, P. (1999). Stability of elemental carbon in a

522 savanna soil total of the soil protected. *Global Biogeochemical Cycles*, *13*, 923–932.

523 Bird, M. I., Veenendaal, E. M., Moyo, C., Lloyd, J., Frost, P. (2000). Effect of fire and soil

524 texture on soil carbon in a sub-humid savanna (Matopos, Zimbabwe). *Geoderma*, *94*,

525 71–90. [https://doi.org/10.1016/S0016-7061\(99\)00084-1](https://doi.org/10.1016/S0016-7061(99)00084-1)

526 Bodí, M. B., Martin, D. A., Balfour, V. N., Santín, C., Doerr, S. H., Pereira, P., Cerda, A., Matáix-

527 Solera, J. (2014). Wildland fire ash: production , composition and eco-hydro-
528 geomorphic effects. *Earth Science Reviews*, 130, 8252.
529 <https://doi.org/10.1016/j.earscirev.2014.07.005>

530 Buurman, P., Van Lagen, B., Velthorst, E. J. (1996). *Manual for soil and water analysis*.
531 Backhuys publishers, Leiden, The Netherlands.

532 Campo, J., Merino, A. (2016). Variations in soil carbon sequestration and their determinants
533 along a precipitation gradient in seasonally dry tropical forest ecosystems. *Global*
534 *Change Biology*, 22, 1942–1956. <https://doi.org/doi:10.1111/gcb.13244>

535 Castaldi, S., de Grandcourt, A., Rasile, A., Skiba, U., Valentini, R. (2010). CO₂, CH₄ and N₂O
536 fluxes from soil of a burned grassland in Central Africa. *Biogeosciences*, 7, 3459–3471.
537 <https://doi.org/10.5194/bg-7-3459-2010>

538 Coetsee, C., Bond, W. J., February, E. C. (2010). Frequent fire affects soil nitrogen and carbon
539 in an African savanna by changing woody cover. *Oecologia*, 162, 1027–1034.
540 <https://doi.org/10.1007/s00442-009-1490-y>

541 Dicen, G. P., Rallos, R. V., Leonard, J., Navarrete, I. A. (2020). Vulnerability of soil organic
542 matter to microbial decomposition as a consequence of burning. *Biogeochemistry*, 1.
543 <https://doi.org/10.1007/s10533-020-00688-1>

544 Fan, Z., Neff, J. C., Hanan, N. P. (2015). Modeling pulsed soil respiration in an African savanna
545 ecosystem. *Agricultural and Forest Meteorology*, 200, 282–292.
546 <https://doi.org/10.1016/j.agrformet.2014.10.009>

547 Feig, G. T. (2004). *The Effect of Fire Regime on Soil Microbial Community Composition and*
548 *Activity*. MSc Thesis, University of the Witwatersrand, Johannesburg.

549 Fritze, H., Smolander, A., Levula, T., Kitunen, V., Mälkönen, E. (1994). Wood-ash fertilization
550 and fire treatments in a Scots pine forest stand: Effects on the organic layer, microbial

551 biomass, and microbial activity. *Biology and Fertility of Soils*, 17, 57–63.
552 <https://doi.org/10.1007/BF00418673>

553 García-Oliva, F., Sanford, R. L., Kelly, E. (1999). Effect of burning of tropical deciduous forest
554 soil in Mexico on the microbial degradation of organic matter. *Plant and Soil*, 206, 29–
555 36. <https://doi.org/10.1023/A:1004390202057>

556 Gómez-Rey, M. X., Madeira, M., Coutinho, J. (2012). Wood ash effects on nutrient dynamics
557 and soil properties under Mediterranean climate. *Annals of Forest Science*, 69, 569–
558 579. <https://doi.org/10.1007/s13595-011-0175-y>

559 Göransson, H., Godbold, D. L., Jones, D. L., Rousk, J. (2013). Bacterial growth and respiration
560 responses upon rewetting dry forest soils: Impact of drought-legacy. *Soil Biology and*
561 *Biochemistry*, 57, 477–486. <https://doi.org/10.1016/j.soilbio.2012.08.031>

562 Hageman, P. L. (2007). *U.S. Geological Survey Field Leach Test for Assessing Water Reactivity*
563 *and Leaching Potential of Mine Wastes, Soils, and Other Geologic and Environmental*
564 *Materials. U.S. Geological Survey Techniques and Methods*. Book 5, Chap. D3, 14 p.
565 <https://doi.org/10.3133/tm5D3>

566 Hilscher, A., Heister, K., Siewert, C., Knicker, H. (2009). Mineralisation and structural changes
567 during the initial phase of microbial degradation of pyrogenic plant residues in soil.
568 *Organic Geochemistry*, 40, 332–342.
569 <https://doi.org/10.1016/j.orggeochem.2008.12.004>

570 Hogg, E. H., Lieffers, V. J., Wein, R. W. (1992). Potential Carbon Losses From Peat Profiles:
571 Effects of Temperature , Drought Cycles, and Fire. *Ecological Society of America*, 2,
572 298–306. <https://doi.org/10.2307/1941863>

573 Irvine, J., Law, B. E., Hibbard, K. A. (2007). Postfire carbon pools and fluxes in semiarid
574 ponderosa pine in Central Oregon. *Global Change Biology*, 13, 1748–1760.
575 <https://doi.org/10.1111/j.1365-2486.2007.01368.x>

576 Jarvis, P., Rey, A., Petsikos, C., Wingate, L., Rayment, M., Pereira, J., Banza, J., David, J.,
577 Miglietta, F., Borghetti, M., Manca, G., Valentini, R. (2007). Drying and wetting of
578 Mediterranean soils stimulates decomposition and carbon dioxide emission: the “Birch
579 effect.” *Tree Physiology*, 27, 929–940.
580 <https://doi.org/https://doi.org/10.1093/treephys/27.7.929>

581 Jensen, M., Michelsen, A., Gashaw, M. (2001). Responses in plant, soil inorganic and
582 microbial nutrient pools to experimental fire, ash and biomass addition in a woodland
583 savanna. *Oecologia*, 128, 85–93. <https://doi.org/10.1007/s004420000627>

584 Jones, D. L., Murphy, D. V., Khalid, M., Ahmad, W., Edwards-Jones, G., DeLuca, T. H. (2011).
585 Short-term biochar-induced increase in soil CO₂ release is both biotically and abiotically
586 mediated. *Soil Biology and Biochemistry*, 43, 1723–1731.
587 <https://doi.org/10.1016/j.soilbio.2011.04.018>

588 Jones, M. W., Santín, C., van der Werf, G. R., Doerr, S. H. (2019). Global fire emissions
589 buffered by the production of pyrogenic carbon. *Nature Geoscience*, 12, 742–747.
590 <https://doi.org/10.1038/s41561-019-0403-x>

591 Khosa, F. V., Mateyisi, M. J., Van Der Merwe, M. R., Feig, G. T., Engelbrecht, F. A., Savage,
592 M. J. (2020). Evaluation of soil moisture from CCAM-CABLE simulation, satellite-based
593 models estimates and satellite observations: A case study of Skukuza and Malopeni flux
594 towers. *Hydrology and Earth System Sciences*, 24, 1587–1609.
595 <https://doi.org/10.5194/hess-24-1587-2020>

596 Longdoz, B., Yernaux, M., Aubinet, M. (2000). Soil CO₂ efflux measurements in mixed forest:
597 impact of chamber disturbance, spatial variability and seasonal evolution. *Global
598 Change Biology*, 6, 907–917. <https://doi.org/10.1046/j.1365-2486.2000.00369.x>

599 Maestrini, B., Nannipieri, P., Abiven, S. (2015). A meta-analysis on pyrogenic organic matter
600 induced priming effect. *GCB Bioenergy*, 7, 577–590.
601 <https://doi.org/10.1111/gcbb.12194>

602 Matáix-Solera, J., Guerrero, C., Garcia-Orenes, F., Barcenas, G. M., Torres, M. P. (2009).
603 Forest fire effects on soil microbiology. In *Fire effects on soils and restoration*
604 *strategies*. <https://doi.org/10.1201/9781439843338-c5>

605 Meigs, G. W., Donato, D. C., Campbell, J. L., Jonathan, G., Law, B. E. (2009). Forest fire
606 impacts on carbon uptake, storage, and emission: the role of burn severity in the
607 Eastern Cascades, Oregon. *Ecosystems*, 12, 1246–1267.
608 <https://doi.org/10.1007/s10021-009-9285-x>

609 Meisner, A., Leizeaga, A., Rousk, J., Bååth, E. (2017). Partial drying accelerates bacterial
610 growth recovery to rewetting. *Soil Biology and Biochemistry*, 112, 269–276.
611 <https://doi.org/10.1016/j.soilbio.2017.05.016>

612 Meisner, A., Rousk, J., Bååth, E. (2015). Prolonged drought changes the bacterial growth
613 response to rewetting. *Soil Biology and Biochemistry*, 88, 314–322.
614 <https://doi.org/10.1016/j.soilbio.2015.06.002>

615 Merino, A., Chávez-Vergara, B., Salgado, J., Fonturbel, M. T., García-Oliva, F., Vega, J. A.
616 (2015). Variability in the composition of charred litter generated by wildfire in different
617 ecosystems. *Catena*, 133, 52–63. <https://doi.org/10.1016/j.catena.2015.04.016>

618 Perkiömäki, J., Kiikkilä, O., Moilanen, M., Issakainen, J., Tervahauta, A., Fritze, H. (2003).
619 Cadmium-containing wood ash in a pine forest: Effects on humus microflora and
620 cadmium concentrations in mushrooms, berries, and needles. *Canadian Journal of*
621 *Forest Research*, 33, 2443–2451. <https://doi.org/10.1139/x03-169>

622 Pinto, A. S., Bustamante, M. M. C., Kisselle, K., Burke, R., Zepp, R., Viana, L. T., Varella, R. F.,
623 Molina, M. (2002). Soil emissions of N₂O, NO, and CO₂ in Brazilian Savannas: Effects of

624 vegetation type, seasonality, and prescribed fires. *Journal of Geophysical Research*,
625 107, 1–9. <https://doi.org/10.1029/2001jd000342>

626 Raison, R. J., McGarity, J. W. (1980). Effects of ash, heat, and the ash-heat interaction on
627 biological activities in two contrasting soils - I. Respiration rate. *Plant and Soil*, 55, 363–
628 376. <https://doi.org/10.1007/BF02182697>

629 Sánchez-García, C., Oliveira, B. R. F., Keizer, J. J., Doerr, S. H., Urbanek, E. (2020). Water
630 repellency reduces soil CO₂ efflux upon rewetting. *Science of the Total Environment*,
631 708. <https://doi.org/10.1016/j.scitotenv.2019.135014>

632 Santín, C., Doerr, S. (2018). Chapter 7 - Carbon. In *Fire effects on soil properties* (pp. 115–
633 128). CSIRO Publishing.

634 Santín, C., Doerr, S. H., Jones, M. H., Merino, A., Warneke, C., Roberts, J. M. (2020). The
635 relevance of pyrogenic carbon for carbon budgets from fires: insights from the FIREX
636 experiment. *Global Biogeochemical Cycles*, (C), 1–17.
637 <https://doi.org/10.1029/2020gb006647>

638 Santín, C., Doerr, S. H., Merino, A., Bryant, R., Loader, N. J. (2016). Forest floor chemical
639 transformations in a boreal forest fire and their correlations with temperature and
640 heating duration. *Geoderma*, 264, 71–80.
641 <https://doi.org/10.1016/j.geoderma.2015.09.021>

642 Santín, C., Doerr, S. H., Merino, A., Bucheli, T. D., Bryant, R., Ascough, P., Gao, X., Masiello, C.
643 A. (2017). Carbon sequestration potential and physicochemical properties differ
644 between wildfire charcoals and slow-pyrolysis biochars. *Scientific Reports*, 7, 1–11.
645 <https://doi.org/10.1038/s41598-017-10455-2>

646 Santín, C., Doerr, S. H., Preston, C. M., González-Rodríguez, G. (2015). Pyrogenic organic
647 matter production from wildfires: a missing sink in the global carbon cycle. *Global
648 Change Biology*, 21, 1621–1633. <https://doi.org/10.1111/gcb.12800>

649 Santín, C., Doerr, S. H., Shakesby, R. A., Bryant, R., Sheridan, G. J., Lane, P. N. J., Smith, H. G.,
650 Bell, T. L. (2012). Carbon loads, forms and sequestration potential within ash deposits
651 produced by wildfire: New insights from the 2009 “Black Saturday” fires, Australia.
652 *European Journal of Forest Research*, 131, 1245–1253.
653 <https://doi.org/10.1007/s10342-012-0595-8>

654 Serrano-Ortiz, P., Roland, M., Sanchez-Moral, S., Janssens, I. A., Domingo, F., Goddérés, Y.,
655 Kowalski, A. S. (2010). Hidden, abiotic CO₂ flows and gaseous reservoirs in the
656 terrestrial carbon cycle: Review and perspectives. *Agricultural and Forest Meteorology*,
657 150, 321–329. <https://doi.org/10.1016/j.agrformet.2010.01.002>

658 Shackleton, C. M., Scholes, R. J. (2000). Impact of fire frequency on woody community
659 structure and soil nutrients in the Kruger National Park. *Koedoe*, 43, 75–81.
660 <https://doi.org/10.4102/koedoe.v43i1.210>

661 Smit, I. P. J., Asner, G. P. (2012). Roads increase woody cover under varying geological,
662 rainfall and fire regimes in African savanna. *Journal of Arid Environments*, 80, 74–80.
663 <https://doi.org/https://doi.org/10.1016/j.jaridenv.2011.11.026>

664 Smith, J. L., Collins, H. P., Bailey, V. L. (2010). The effect of young biochar on soil respiration.
665 *Soil Biology and Biochemistry*, 42, 2345–2347.
666 <https://doi.org/10.1016/j.soilbio.2010.09.013>

667 Spohn, M., Schleuss, P. M. (2019). Addition of inorganic phosphorus to soil leads to
668 desorption of organic compounds and thus to increased soil respiration. *Soil Biology*
669 *and Biochemistry*, 130, 220–226. <https://doi.org/10.1016/j.soilbio.2018.12.018>

670 Stockmann, U., Adams, M. A., Crawford, J. W., Field, D. J., Henakaarchchi, N., Jenkins, M.,
671 Minasny, B., McBratney, A. B., de Courcelles, V. R., Singh, K., Wheeler, I., Abbott, K.,
672 Angers, D. A., Baldock, J., Bird, M., Brookes, P. C., Chenu, C., Jastrow, J. D., Lal, R.,

673 Lehmann, J., O'Donnell, A. G., Parton, W. J., Whitehead, D., Zimmermann, M. (2013).
674 The knowns, known unknowns and unknowns of sequestration of soil organic carbon.
675 *Ecosystems and Environment*, 164, 80–99.
676 <http://dx.doi.org/10.1016/j.agee.2012.10.001>

677 Thomas, A. D., Dougill, A. J., Elliott, D. R., Mairs, H. (2014). Seasonal differences in soil CO₂
678 efflux and carbon storage in Ntwetwe Pan, Makgadikgadi Basin, Botswana. *Geoderma*,
679 219–220, 72–81. <https://doi.org/10.1016/j.geoderma.2013.12.028>

680 Van Der Werf, G. R., Randerson, J. T., Giglio, L., Van Leeuwen, T. T., Chen, Y., Rogers, B. M.,
681 Mu, M., Van Markle, M. J. E., Morton, D. C., Collatz, G. J., Yokelson, R. J., Kasibhatla, P.
682 S. (2017). Global fire emissions estimates during 1997-2016. *Earth System Science*
683 *Data*, 9, 697–720. <https://doi.org/10.5194/essd-9-697-2017>

684 van Straaten, O., Doamba, S. W. M. F., Corre, M. D., Veldkamp, E. (2019). Impacts of burning
685 on soil trace gas fluxes in two wooded savanna sites in Burkina Faso. *Journal of Arid*
686 *Environments*, 165, 132–140. <https://doi.org/10.1016/j.jaridenv.2019.02.013>

687 Vargas, R., Collins, S. L., Thomey, M. L., Johnson, J. E., Brown, R. F., Natvig, D. O., Friggens, M.
688 T. (2012). Precipitation variability and fire influence the temporal dynamics of soil CO₂
689 efflux in an arid grassland. *Global Change Biology*, 18, 1401–1411.
690 <https://doi.org/10.1111/j.1365-2486.2011.02628.x>

691 Wei, F., Wang, S., Fu, B., Brandt, M., Pan, N., Wang, C., Fensholt, R. (2020). Nonlinear
692 dynamics of fires in Africa over recent decades controlled by precipitation. *Global*
693 *Change Biology*, 26, 4495–4505. <https://doi.org/10.1111/gcb.15190>

694 Whitman, T., Pepe-Rannek, C., Enders, A., Koechli, C., Campbell, A., Buckley, D. H., Lehmann,
695 J. (2016). Dynamics of microbial community composition and soil organic carbon
696 mineralization in soil following addition of pyrogenic and fresh organic matter. *ISME*
697 *Journal*, 10, 2918–2930. <https://doi.org/10.1038/ismej.2016.68>

698 Wüthrich, C., Schaub, D., Weber, M., Marxer, P., Conedera, M. (2002). Soil respiration and
699 soil microbial biomass after fire in a sweet chestnut forest in southern Switzerland.
700 *Catena*, *48*, 201–215. [https://doi.org/10.1016/S0341-8162\(01\)00191-6](https://doi.org/10.1016/S0341-8162(01)00191-6)

701 Zepp, G., Miller, L., Burke, A., Parsons, D. A. B., Scholes, M. C., Service, P. (1996). Effects of
702 moisture and burning on soil-atmosphere exchange of trace carbon gases in a southern
703 African savanna. *Journal of Geophysical Research*, *101*, 23699–23706.
704 <https://doi.org/10.1029/95JD01371>

705 Zimmermann, M., Bird, M. I., Wurster, C., Saiz, G., Goodrick, I., Barta, J., Capek, P.,
706 Santruckova, H., Smernik, R. (2012). Rapid degradation of pyrogenic carbon. *Global*
707 *Change Biology*, *18*, 3306–3316. <https://doi.org/10.1111/j.1365-2486.2012.02796.x>

708 Zimmermann, S., Frey, B. (2002). Soil respiration and microbial properties in an acid forest
709 soil: Effects of wood ash. *Soil Biology and Biochemistry*. [https://doi.org/10.1016/S0038-](https://doi.org/10.1016/S0038-0717(02)00160-8)
710 [0717\(02\)00160-8](https://doi.org/10.1016/S0038-0717(02)00160-8)

711 Zubkova, M., Boschetti, L., Abatzoglou, J. T., Giglio, L. (2019). Changes in Fire Activity in
712 Africa from 2002 to 2016 and Their Potential Drivers. *Geophysical Research Letters*, *46*,
713 7643–7653. <https://doi.org/10.1029/2019GL083469>

714

715

716

Table 1. Experimental fire characteristics including atmospheric conditions (wind speed, air temperature (Air T) and relative humidity (RH)), pre-fire soil water content (SWC), maximum temperature range (Tmax) registered in the soil surface and grass (n = 12), temperature residence times > 300 °C, and details of fire impacts on vegetation. Full details of temperatures reached during the experimental fires and their residence times in the soil surface and grass are provided in Supplementary Table 1.

Site	Date	Atmospheric conditions			SWC (% grav.)	T max (°C)		T residence time > 300 °C (s)*		Fire impacts on vegetation
		Wind speed (m s ⁻¹)	Air T (°C)	RH (%)		Soil surface	Grass	Soil surface	Grass	
PB1	19/08/18	1.8 – 2.7	26	41	3.6 ± 0.7	40 - 225	484 – 744	0	23 ± 20	In both PB1 and PB3 the fire burnt the entire experimental plot with complete combustion of fine fuels and no unburnt grass left. Woody fuels were mostly unaffected and wood on the ground (down wood) and bark from standing trees remained uncharred. Most (> 90%) of the fine fuels on the ground were burnt. Coarser woody fuels remained largely unaffected, whereas most of the green and brown leaves of the shrubs were consumed.
PB3	19/08/18	1.8 – 2.7	31	30	5.1 ± 1.9	40 - 182	651- 918	0	54 ± 38	
MB1	23/08/18	2.2 – 3.1	31	41	2.0 ± 0.3	40 - 498	452 - 850	15 ± 24	51 ± 40	

* Reported as this is the temperature threshold above which organic materials tend to transform into more aromatic and recalcitrant forms (Santín et al., 2016).

Table 2. Carbon (C) respired as CO₂ (CO₂-C; g C m⁻²) during the 28-day observation period and during the CO₂ pulse (lasting 34 - 130 h) in g of C and as a percentage of the total C (TC). Values are the arithmetic mean (n = 3) with standard deviation.

		Total CO ₂ -C released - entire observation (g C m ⁻²)	CO ₂ -C released - entire observation (g)	CO ₂ -C released - pulse only (g)	CO ₂ -C released - entire observation (% of TC)	CO ₂ -C released - pulse only (% of TC)
PB1	PreF	9.8 ± 0.6	0.065 ± 0.004	0.007 ± 0.001	7.9 ± 0.4	0.8 ± 0.1
	PostF	12.3 ± 0.4	0.082 ± 0.002	0.029 ± 0.002	7.8 ± 0.3	2.8 ± 0.2
	PostF_wA	20.5 ± 1.2	0.136 ± 0.008	0.056 ± 0.006	5.4 ± 0.3	2.2 ± 0.2
PB3	PreF	7.4 ± 0.3	0.049 ± 0.002	0.011 ± 0.001	4.5 ± 0.2	1.0 ± 0.1
	PostF	14.6 ± 0.3	0.097 ± 0.002	0.032 ± 0.004	6.4 ± 0.1	2.1 ± 0.3
	PostF_wA	21.3 ± 0.7	0.142 ± 0.004	0.043 ± 0.002	4.8 ± 0.2	1.4 ± 0.1
MB1	PreF	9.5 ± 0.2	0.063 ± 0.001	0.010 ± 0.001	3.1 ± 0.1	0.5 ± 0.1
	PostF	12.9 ± 0.8	0.086 ± 0.005	0.021 ± 0.004	3.8 ± 0.2	1.0 ± 0.2
	PostF_wA	20.6 ± 0.8	0.137 ± 0.005	0.032 ± 0.001	3.3 ± 0.1	0.7 ± 0

Table 3. Spearman's rank correlation (Spearman's rho) between CO₂ flux (size of the pulse and cumulative flux) and selected characteristics of the PreF, PostF and PostF_wA samples in mg kg⁻¹ (total C and N, and dissolved organic carbon (DOC), NH₄⁺, NO₃⁻² and PO₄⁻³; n = 9). Values with an asterisk show significant differences (at p < 0.05).

	Size of CO ₂ pulse (μmol m ⁻² s ⁻¹)	Cumulative CO ₂ flux (mmol m ⁻²)	TC (g kg ⁻¹)	TN (g kg ⁻¹)	DOC (mg kg ⁻¹)	NH ₄ ⁺ (mg kg ⁻¹)	NO ₃ ⁻² (mg kg ⁻¹)	PO ₄ ⁻³ (mg kg ⁻¹)
Size of CO ₂ pulse (μmol m ⁻² s ⁻¹)	1.000							
Cumulative CO ₂ flux (mmol m ⁻²)	0.917*	1.000						
TC (g kg ⁻¹)	0.667*	0.767*	1.000					
TN (g kg ⁻¹)	0.350	0.433	0.85*	1.000				
DOC (mg kg ⁻¹)	0.833*	0.95*	0.633	0.317	1.000			
NH ₄ ⁺ (mg kg ⁻¹)	0.717*	0.600	0.133	-0.133	0.617	1.000		
NO ₃ ⁻² (mg kg ⁻¹)	0.067	0.017	0.500	0.717*	-0.167	-0.083	1.000	
PO ₄ ⁻³ (mg kg ⁻¹)	0.583	0.667*	0.867	0.714	0.733	0.150	0.283	1.000

Table 4. Chemical properties of the pre-fire (PreF) and post-fire (PostF) soils and of the ash. Values are the arithmetic mean (n = 3) with standard deviation. Values with an asterisk show significant differences (at p < 0.05) between pre- and post-fire soil.

		pH	EC ($\mu\text{S cm}^{-1}$)	DOC (mg kg^{-1})	NH ₄ ⁺ (mg kg^{-1})	NO ₃ ⁻² (mg kg^{-1})	PO ₄ ⁻³ (mg kg^{-1})
PB1	PreF	6.4 ± 0.2	60.2 ± 25.8	8.4 ± 3.4	0.2 ± 0	0.4 ± 0.1	0.5 ± 0.3
	PostF	7.0 ± 0.5	99.7 ± 24.9	13.7* ± 1.5	0.7 ± 0.4	0.8* ± 0.2	1.2 ± 0.7
	Ash	9.8 ± 0.2	5543.3 ± 605.8	100.4 ± 36.1	0.5 ± 0.1	4.7 ± 1.3	6.7 ± 2.7
PB3	PreF	6.7 ± 0.1	68.9 ± 39	5.0 ± 3.1	0.1 ± 0	0.7 ± 0.2	0.5 ± 0
	PostF	7.5* ± 0.5	206.4* ± 37.1	27.2* ± 9.3	0.6* ± 0.2	0.4 ± 0.2	2.3* ± 0.3
	Ash	10.0 ± 0.1	4776.7 ± 631.7	84.4 ± 12.2	0.4 ± 0	3.2 ± 0.4	6.2 ± 1.7
MB1	PreF	7.9 ± 0.1	139.4 ± 22.2	5.7 ± 1.9	0.1 ± 0	1.5 ± 0.4	2.0 ± 0.5
	PostF	7.6 ± 0.4	258.0* ± 43.7	19.4* ± 5	0.2 ± 0.1	0.9* ± 0.1	2.4 ± 0.6
	Ash	9.9 ± 0	2877.7 ± 965.3	50.3 ± 2.2	0.2 ± 0	1.6 ± 0.3	149.3 ± 29.9

Table 5. Elemental concentrations (mg kg⁻¹) for the pre-fire (PreF) and post-fire (PostF) soil and the ash. Values are the arithmetic mean (n = 3) with standard deviation. Values with an asterisk show significant differences (at p < 0.05) between pre and post-fire soil.

		C:N	TC	TN	Al	Ca	Co	Cr	Cu	Fe	Mg	Mn	Ni	P	Zn
PB1	PreF	16 ± 3	11797 ± 5100	750 ± 400	14449 ± 2821	481 ± 337	4 ± 1	40 ± 3	6 ± 1	14732 ± 1766	356 ± 96	193 ± 42	2 ± 1	97 ± 34	11 ± 2
	PostF	16 ± 4	14963 ± 1000	943 ± 200	14643 ± 1530	723 ± 93	4 ± 0	25* ± 1	8* ± 0	18219 ± 2672	393 ± 64	218 ± 3	2 ± 1	125 ± 31	11 ± 1
	Ash	39 ± 2	248267 ± 45700	6287 ± 1000	9852 ± 1530	34226 ± 1262	19 ± 1	51 ± 13	32 ± 1	6551 ± 1521	7373 ± 420	1297 ± 58	8 ± 1	3902 ± 272	164 ± 13
PB3	PreF	16 ± 0	15730 ± 6000	990 ± 400	12601 ± 3703	999 ± 662	5 ± 2	59 ± 3	7 ± 1	10656 ± 954	397 ± 105	244 ± 34	8 ± 3	128 ± 19	11 ± 2
	PostF	19 ± 3	21543 ± 13300	1147 ± 600	10867 ± 668	1419 ± 607	4 ± 1	41* ± 6	8 ± 1	9735 ± 1646	482 ± 64	246 ± 13	8 ± 1	149 ± 22	9 ± 3
	Ash	50 ± 3	208967 ± 16800	4203 ± 600	9917 ± 2709	43281 ± 4976	8 ± 11	65 ± 17	29 ± 9	7256 ± 2007	8936 ± 1026	1435 ± 252	14 ± 3	4687 ± 515	182 ± 27
MB1	PreF	15 ± 0	29050 ± 1100	1977 ± 100	36248 ± 1406	17700 ± 666	37 ± 1	353 ± 15	75 ± 1	57773 ± 1277	20740 ± 651	949 ± 3	348 ± 8	1217 ± 84	78 ± 1
	PostF	16 ± 1	31850 ± 5500	2047 ± 400	35153 ± 2200	16606 ± 1126	38 ± 1	353 ± 8	77 ± 4	57298 ± 945	21135 ± 192	941 ± 29	349 ± 8	1437* ± 71	164 ± 13
	Ash	93 ± 5	286133 ± 6500	3080 ± 100	3695 ± 329	17870 ± 2724	4 ± 1	57 ± 1	22 ± 1	6125 ± 430	6872 ± 590	252 ± 21	44 ± 2	5861 ± 1040	129 ± 15

Table 6. Main TG-DSC parameters for the pre-fire (PreF) and post-fire soil (PostF) and in the ash. T50_Q: temperature at which the sample released half of its total stored energy; Q1, Q2 and Q3: percentage of heat released in each group of thermal oxidation (150 – 375 °C; 375 – 475 °C; 475 – 600 °C respectively). Values are the arithmetic mean (n = 3) with standard deviation.

Site	Treatment	T50 _Q (°C)	Q1 (%)	Q2 (%)	Q3 (%)
PB1	PreF	371.3 ± 25.9	44.9 ± 12.6	31.7 ± 6.6	23.3 ± 9.5
	PostF	387.7 ± 27.1	42.1 ± 10.3	34.7 ± 7.7	23.2 ± 18
	Ash	414.3 ± 2.6	29.4 ± 1.4	55.9 ± 1.1	14.6 ± 1.9
PB3	PreF	304.0 ± 133.5	40.9 ± 0.7	35.9 ± 8	23.2 ± 7.7
	PostF	355.0 ± 35.5	53.0 ± 12.4	35.2 ± 9.8	11.8 ± 4.1
	Ash	419.0 ± 3.2	26.3 ± 2.6	56.4 ± 0.2	17.3 ± 2.5
MB1	PreF	342.0 ± 1.7	53.6 ± 2.6	33.2 ± 1.6	13.1 ± 4.3
	PostF	343.0 ± 3.6	53.3 ± 2.8	33.7 ± 0.4	13.0 ± 2.9
	Ash	433.8 ± 4.4	21.2 ± 2.6	53.4 ± 1.6	25.4 ± 3.5

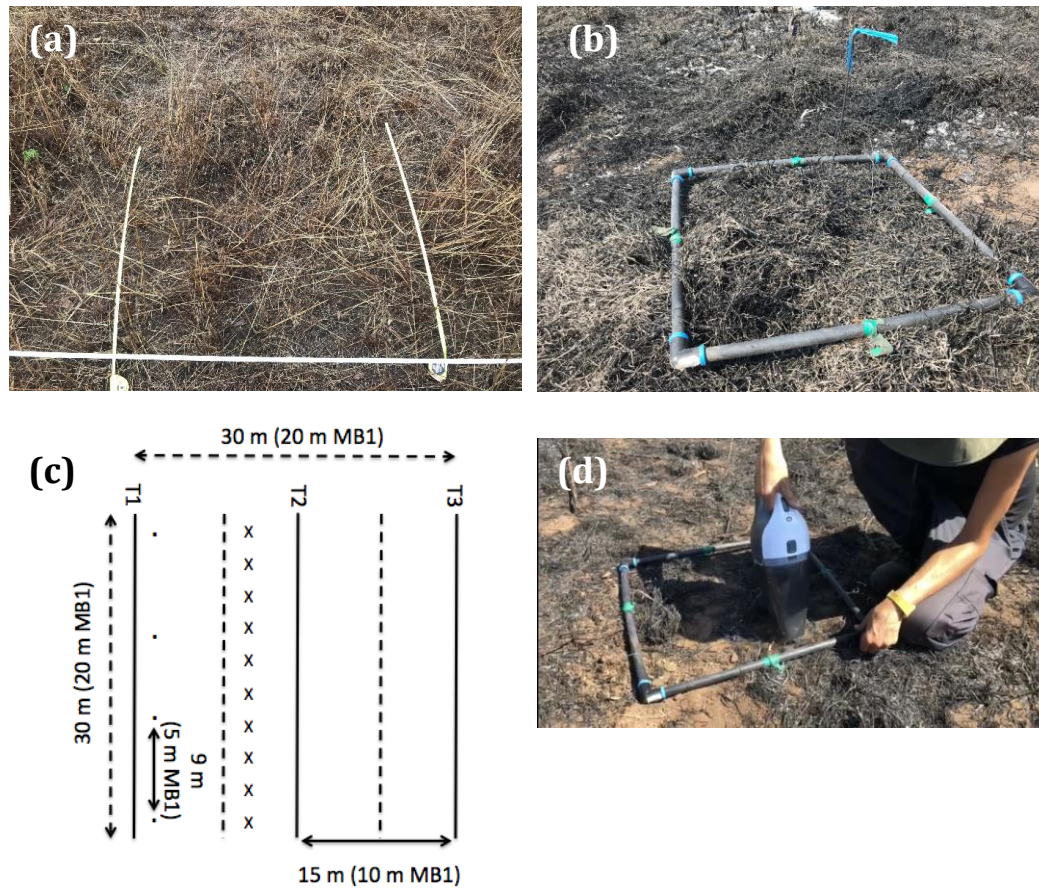


Fig. 1. **(A)** Grass in the PB3 site before the fire. **(B)** Burnt grass in the MB1 site after the fire. **(C)** Experimental plot diagram for PB1 and PB3 plots, and dimensions for the MB1 plot in brackets. Solid lines represent the experimental transects and dashed lines represent the control transects. Dots along the experimental transects represent the locations of the thermocouples and crosses along the control transect represent soil sampling locations before the fire. **(D)** Sampling the ash layer in the MB1 site after the fire.

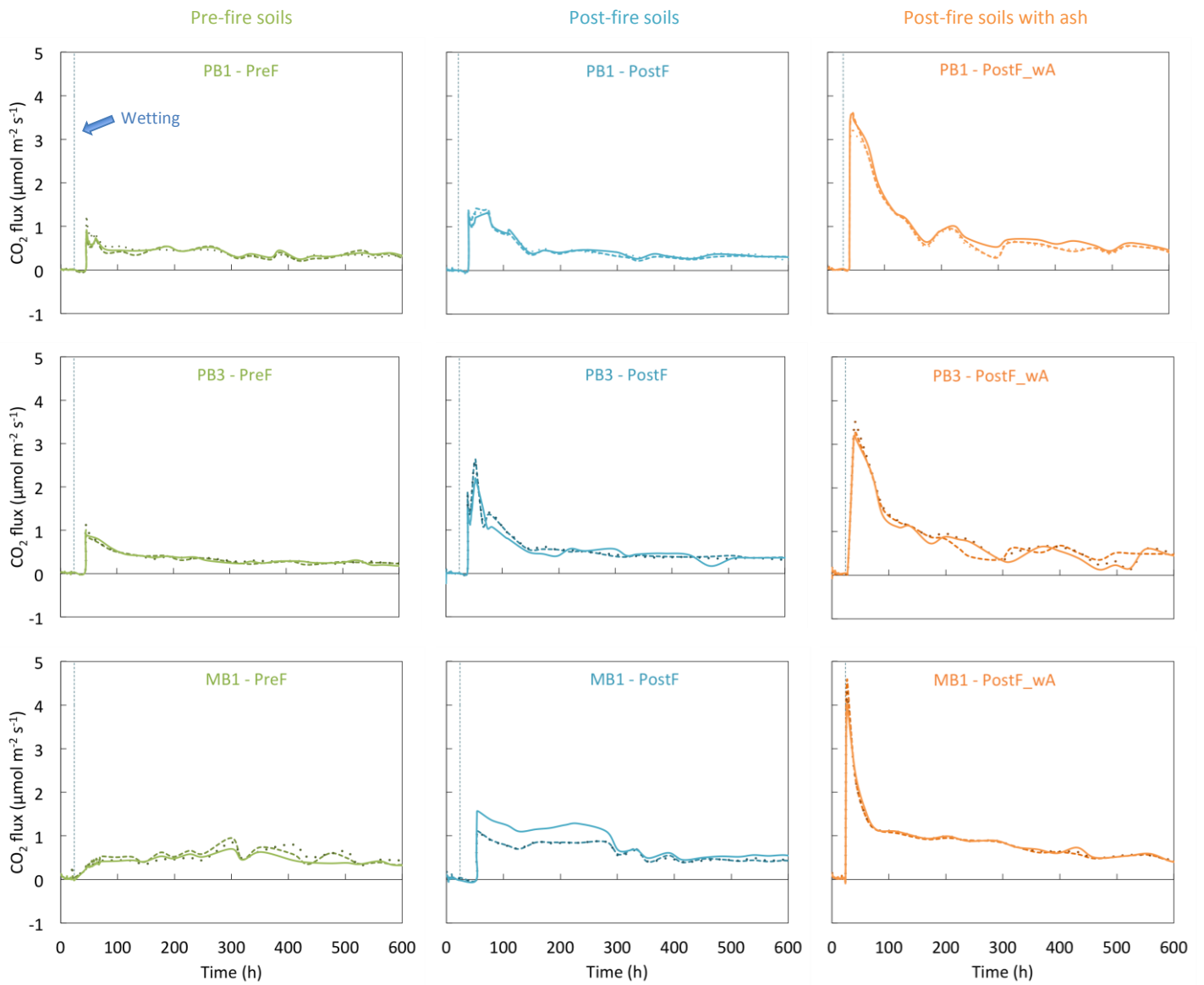


Fig. 2. Response of CO₂ flux to wetting of pre- (PreF) and post-fire soils (PostF) and post-fire soils with added ash (PostF_wA). Solid, dotted and dashed lines represent the three replicates. The blue dashed vertical line represents the start of the wetting, 24 h after the start of measurements.

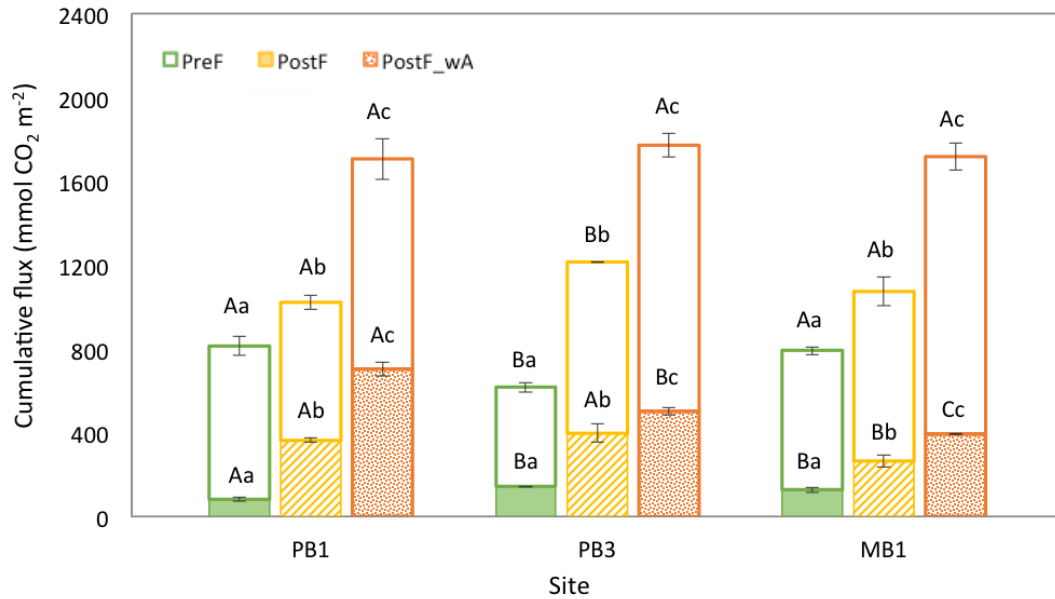


Fig. 3. Cumulative flux for the duration of the observations (28 d) (total columns) and proportion of the cumulative flux released only during the CO₂ pulse (24 – 130 h) (filled columns) in the pre-fire (PreF) and post-fire soils (PostF) and in the post-fire soils with added ash (PostF_wA). Values represent the mean (n = 3) with standard deviation bars. Different lowercase letters (a – c) within the same site indicate significant differences between incubation treatments and different uppercase letters (A – C) indicate significant differences between sites for each treatment at p < 0.05. Letters above the unfilled columns represent differences between the total cumulative flux and letters above the filled columns represent differences between the cumulative flux released during the CO₂ pulse.

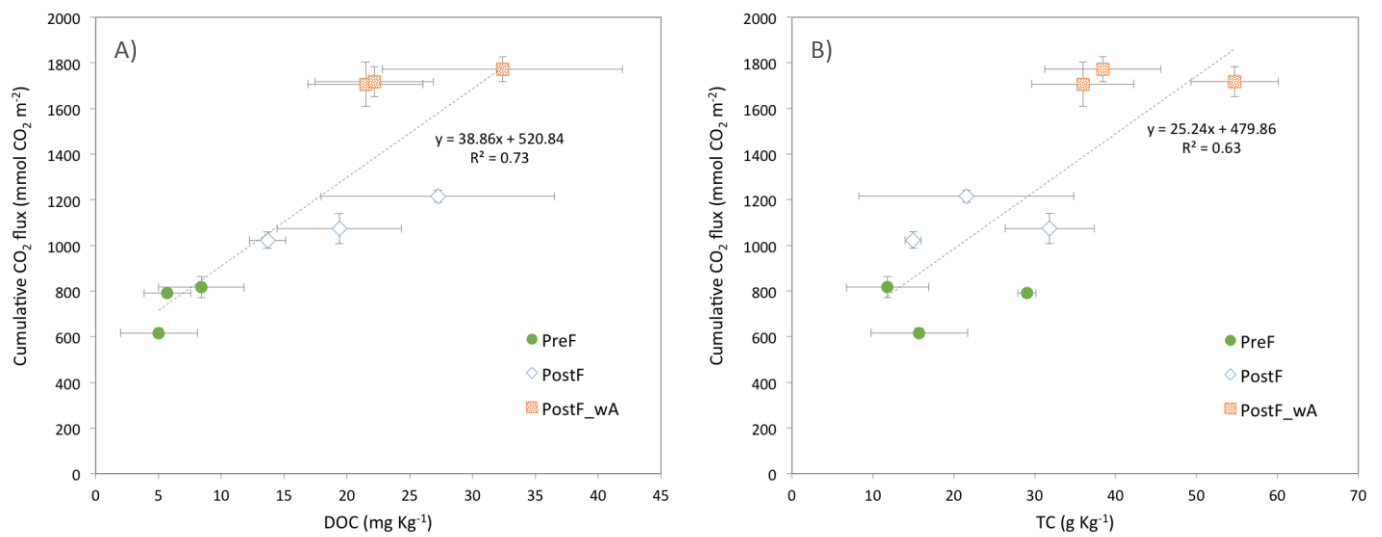


Fig. 4. A) Relationship between cumulative CO₂ flux and dissolved organic carbon (DOC) ($p < 0.001$) and B) relationship between cumulative CO₂ flux and total carbon (TC) ($p < 0.05$) in the pre-fire (PreF) and post-fire soils (PostF) and in the post-fire soils with added ash (PostF_wA). Values are the arithmetic mean ($n = 3$) with standard deviation bars.



[Click here to access/download](#)

Supplementary Material for online publication only
SupInfo.docx



Conflict of interest statement

The authors have no conflict of interest to declare.